Semi-automated cardiac segmentation on cine magnetic resonance images using GVF-Snake deformable models

Constantin Constantinides[1, 2], Yasmina Chenoune[1, 2], Nadjia Kachenoura[1], Elodie Roullot[2], Elie Mousseaux[3], Alain Herment[1], Frederique Frouin[1]

1- Inserm UMR_S 678; UPMC, 91 Boulevard de l'Hopital, 75013 Paris
2- ESME-SUDRIA, Equipe PRIAM, 38 rue Molière, 94200 Ivry sur Seine
3- AP-HP, HEGP, Service de Radiologie Cardiovasculaire, 20 rue Leblanc, 75015 Paris

Abstract. The segmentation of left ventricular structures is necessary for the evaluation of the ejection fraction (EF) and the myocardial mass (LVM). A semi-automated 2D algorithm using connected filters and a deformable model allowing an accurate endocardial detection was proposed. The epicardial border was deduced using a deformable model restricted inside a region of interest defined from the endocardial border. Papillary muscles were detected using a fuzzy k-means algorithm. The method was applied to the challenge training and validation databases, consisting of 15 subjects each. The evaluation was performed using the tools provided by the challenge. For both datasets, results show a mean Dice metric of 0.89 for endocardial borders (0.92 for epicardial borders). Overall average perpendicular distance was 2.2 mm. Very good correlation was obtained for the EF and LVM parameters. Visual overall rating given by the challenge's cardiologist was 1.2. Segmentation was robust and performed successfully on both datasets.

Keywords. Segmentation, deformable models, morphological filters, cine MRI, evaluation

1 Introduction

Most cardiac pathologies, particularly ischemic heart disease, involve the left ventricle. The clinical evaluation of left ventricular (LV) functions requires the qualitative and/or quantitative analysis of global and regional functions. Cine magnetic resonance imaging (MRI) is considered as the modality of choice for the assessment of the LV ejection fraction (EF) and the LV myocardial mass (LVM). The relevance of these parameters depends on the accuracy of the delimitation of the left ventricular endocardial and epicardial borders. Moreover, the inclusion of papillary muscles inside the cavity or in the myocardial mass is still under debate. This segmentation, when achieved manually, is of course time-consuming and the inter- and intra-observers variability is relatively high. This fact supports the need for some automation. Despite the high number of segmentation approaches that have been proposed, a comparison of different methods on the same dataset and using the same evaluation criteria was lacking. Moreover, the ground truth for evaluation purposes is still under discussion, even if the drawing by an expert can be considered in a first approach as a “gold” standard. Thus this challenge provides a first step towards a thorough and objective evaluation. Our group has recently proposed a 2D LV segmentation algorithm, which was dedicated to the endocardial segmentation and was applied to end-diastolic images in order to have a regional estimation of mean transition times and endocardial velocities [1]. This algorithm is a combination of morphological filters and deformable contours, for which a robust setting of the different parameters was proposed. For this challenge, this method was adapted to systolic endocardial contours, and diastolic epicardial contours. A first attempt to segment papillary muscles was implemented. Finally, the proposed contours were validated or refined by an operator using a dedicated user-friendly graphical interface.

2 Materials and Methods

2.1 Imaging Protocol and Datasets

Cine MR short-axis (SAX) images were obtained with a 1.5T GE Signa MRI. All images were obtained with a temporal resolution of 20 phases over the cardiac cycle. Acquisition was triggered from the end-diastolic phase. Six to twelve SAX slices from the atrioventricular ring to the apex were obtained, (slice thickness = 8 mm, gap = 8 mm, FOV = 320 mm x 320 mm, matrix= 256 x 256 pixels) [2].

	HF-I	**HF-NI**	**HYP**	**N**
Training set	*1 -4*	*5-8*	*9-12*	*13-15*
Validation set	*16 -19*	*20-23*	*24-27*	*28-30*

Table 1. Structuring of training and validation datasets (HF-I = Ischemic Heart Failure; HF-NI = Non-Ischemic Heart Failure; HYP = Hypertrophy; N = Normal).

Two datasets, a training dataset and a validation dataset were provided to the participants in the MICCAI Grand Challenge, by Sunnybrook Health Sciences Centre. Each dataset contains 3 healthy subjects and 3 groups of 4 subjects with different pathologies (Table 1). Ground truth was provided to the participating teams for the end-diastolic (ED) and end-systolic (ES) phases for the training dataset. Further details on datasets and the acquisition protocol can be found in [3].

2.2 Methods

2.2.1 Segmentation of the endocardium

The segmentation is based on previous works detailed in [1] and [4]; it proceeds in three main steps. The first step consists in defining a region of interest (ROI) by manually positioning a point P0 at the center of the LV and a point P1 at the upper insertion between the LV and the right ventricle (RV). Secondly, a morphological filter that combines openings and closings on connected sets [5] is applied to the ROI, providing an image with homogeneous regions. The number and size of these regions depend on a size parameter λ. Images are filtered with the value of λ that varies from 5% to 80% of the ROIs surface. The ratio between the filtered surface including P0 and λ is computed for each filtered image and the one with the ratio closest to 1 is defined as the default filtered image. The user can either accept it, or refine the value of λ and thus choose another filtered image. Once the best filtered image has been chosen, the third step consists in segmenting the ventricle using P0 as an initialization of the GVF-Snake [6]. The GVF-Snake parameters are similar to those defined in [4]. Figure 1 shows an example of the above described steps and the resulting endocardial contour.

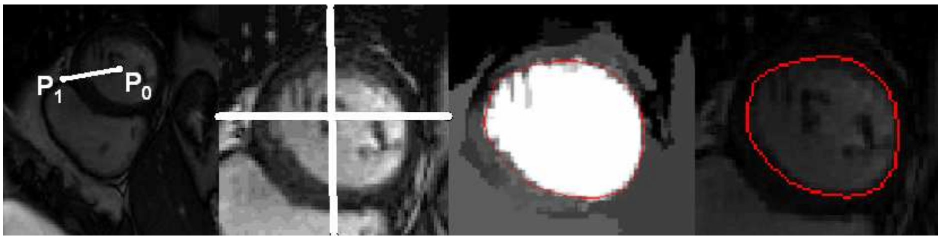

Fig. 1. Illustration of all the steps of an endocardial border segmentation (Subject: SC-HYP-37). From left to right: definition of P0 and P1; definition of the ROI around the LV; filtered image with optimal λ value; resulting segmentation of the endocardium.

2.2.2 Segmentation of the epicardium

The epicardial border is difficult to segment because of the low contrast between the myocardium and surrounding structures. Thus, it appeared necessary to restrain the GVF-Snake evolution within a limited area (Fig. 2-middle) derived from the endocardial border using geometrical considerations such as the expected thickness of the myocardium. The GVF-Snake is initialized with the obtained endocardial border and its default parameters were similar to those of the endocardium except the pressure forces attenuated with successive iterations of the GVF-Snake. This decreasing feature of the pressure forces is chosen to avoid: 1) attraction of the processed contour by the endocardium during the first iterations, and 2) attraction by the external structures.

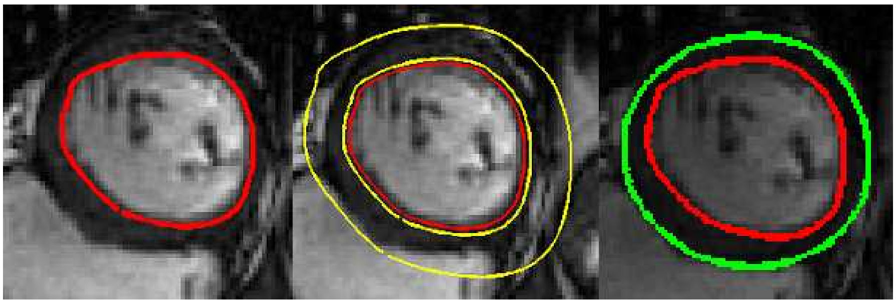

Fig. 2. Illustration of an epicardial border detection (Subject: SC-HYP-37) left: initialization with endocardium; middle: restraining mask (yellow) with endocardial border (red); right: resulting epicardium (green) and endocardium (red).

2.2.3 Detection of papillary muscles (PM)

This is achieved using a fuzzy k-means algorithm [7] applied only within the previously segmented endocardial region. The fuzzy k-means clustering is thus expected to classify between PM regions (dark) and non-PM regions (enhanced). After classification, all pixels that have a probability of membership to the PM region lower than 0.6 are set to zero. Due to the presence of small trabeculations around the LV cavity, the resulting image is eroded. It is then filtered with a median filter (3 x 3) to eliminate the small non-connected regions related to flow effects inside the LV cavity. Structures with the largest areas are proposed as PM. Figure 3 illustrates the PM detection via fuzzy k-means clustering.

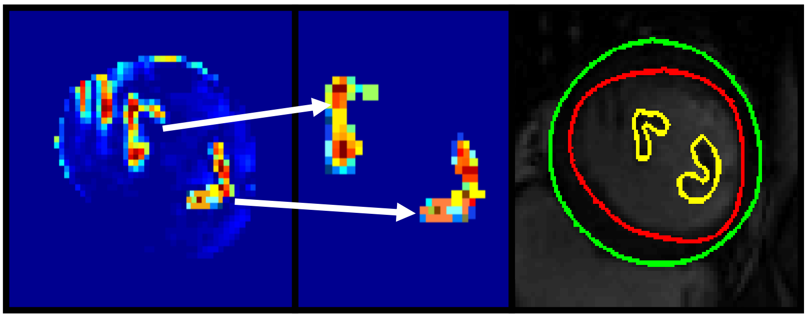

Fig. 3. Left: map of membership to PM regions after fuzzy k-means clustering on the endocardial region; middle: zoomed PM isolation via threshold erosion and median filtering; right: final result (Subject: SC-HYP-37).

2.2.4 Evaluation criteria

Evaluation was based on the delineation of the contours made by an expert cardiologist. The accuracy of the contours provided by the automated segmentation was evaluated using the Dice metric (DM) and the average perpendicular distance (AVP). Moreover, EF and LVM were deduced from automated results and were compared to the expertise. A visual scoring was given by the organizing committee to each participant on the validation dataset. Evaluation tools were common for all participants of the challenge and were fully described in [3].

3 Results

Segmentation was achieved successfully in all cases except for subjects SC-HYP-01, SC-HYP-38, SC-HYP-08 and SC-HF-I-08, where one or two apical slices were removed in systole since they were difficult to segment (with a reduced cavity area). Also, for these same subjects, some epicardial contours were excluded as well because slices were too basal as the amount of myocardium seen was less than 50% of its total surface. The values of the mean "good" percentage (a contour is considered “good” if its AVP is lower than 5mm) obtained for the endocardial and the epicardial borders were respectively:

– 88.41% ±10.17 and 92.89% ± 6.51 for the training dataset
– 92.28% ± 6.05 and 92.22% ± 5.02 for the validation dataset

As the comparison of DM and AVP obtained for both training and validation datasets showed no statistical significance (Student’s t-test), results of both datasets were merged.

Figure 4 shows the average perpendicular distance (AVP) and the average Dice metric (ADM) for each patient, patients being numbered as in Table 1.

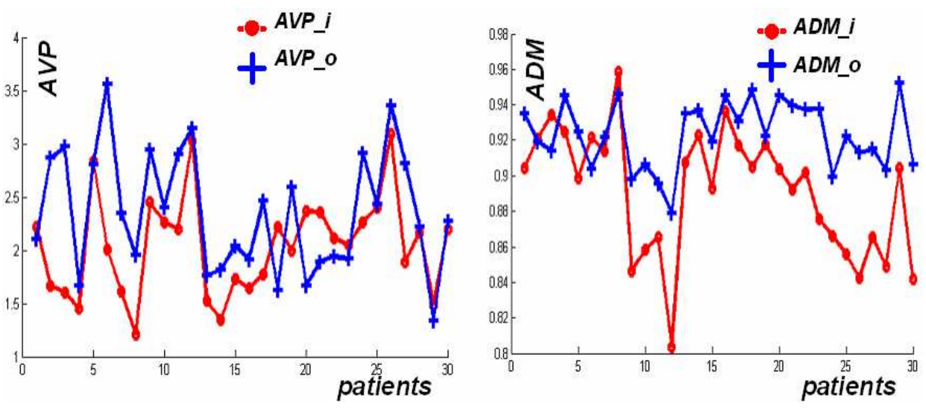

Fig. 4. AVP and ADM for the 30 subjects, endocardium in red, epicardium in blue

The mean AVP for endocardial borders was 2.04 mm ± 0.47 and 2.35 mm ± 0.57 for epicardial borders and it was mostly lower for the endocardium than for the epicardium. It was the lowest for normal subjects (N) (mean AVP_i was 1.74 mm ± 0.36 and mean AVP_o was 1.90 mm ± 0.34) and subjects with ischemic heart failure (HF-I) (mean AVP_i was 1.82 mm ± 0.29 and mean AVP_o was 2.32 mm ± 0.52).

The mean ADM for endocardial borders was 0.89 ± 0.04 and 0.92 ± 0.02 for epicardial borders. The lowest ADM is obtained for one case with hypertrophy (0.8). For both datasets and both contours, our minimal AVP corresponds to the maximum ADM.

Furthermore, comparisons were performed on EF and LVM basis, papillary muscles being either included inside the myocardium (PIM) or inside the cavity (PIC). Results show a good correlation with ground truth for EF independently of papillary muscle inclusion. Equation 1 and figure 5 show the linear regression of the EF and the LVM:

$$\begin{gathered}\text{EF with PIC: } Y = 1.00X + 1.60,\ r^2=0.97\ . \\ \text{EF with PIM: } Y = 1.02X + 1.00,\ r^2=0.96\ . \\ \text{LVM with PIC: } Y = 0.80X + 31.51,\ :\ r^2=0.88. \\ \text{LVM with PIM: } Y = 0.82X + 30.02,\ r^2=0.89\ \ .\end{gathered} \tag{1}$$

where X contains the ground truth values and Y the estimated data.

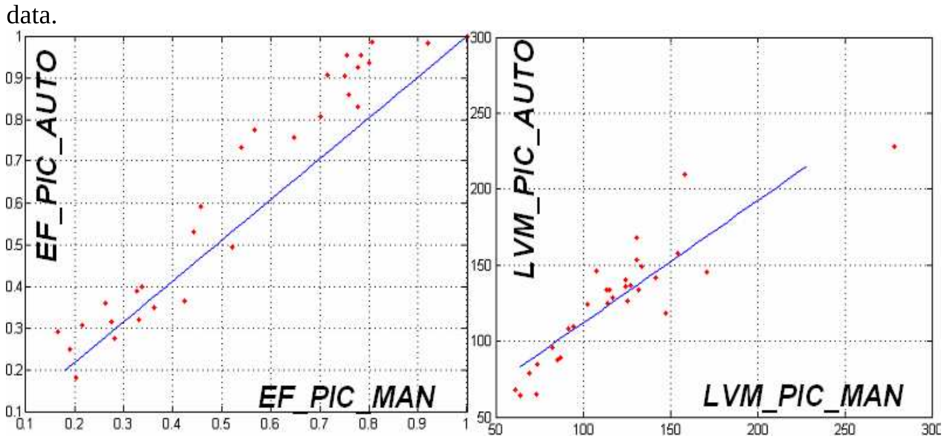

Fig. 5. Linear regression for EF and LVM with PIC: automated (y-axis) vs. ground truth (x-axis).

A visual assessment was made for each subject of both datasets for all slices. The largest differences between manual and automated endocardial contours occurred in apical slices. Furthermore, the organizing committee of the challenge provided visual evaluation results (on the validation dataset only) based on one expert's opinion, a cardiologist. A scale from 1 (excellent contours where only little correction is required) to 4 (subjects contours are unusable) was given. Thirteen subjects got a rating of 1 and two subjects (SC-HF-I-05 and SC-HF-NI-07) got a rating of 2, meaning that more than 50% of the contours are acceptable for these subjects. In the case of subjects with hypertrophy (SC-HYP-08, SC-HYP-37), some systolic and diastolic slices were a bit unmatched with the manual contours. Also, a difficulty with accurate placement of the contours around the LV outflow tract (LVOT) was shown for subjects with hypertrophy and non-ischemic heart-failure as well as for one healthy subject (SC-HYP-08, SC-HF-NI-07 and SC-N-06).

4 Discussion

An accurate estimation of the EF and LV mass is essential for the evaluation of LV function in clinical routine. In this paper a robust and semi-automated segmentation was presented and successfully tested on 30 subjects including patients with various pathologies. Our technique has been successfully used on 20 normal subjects in a previous study [1]. However, only the endocardium was segmented in this study. Our present study aimed at extending the segmentation technique to the epicardium and at reducing computational time. Indeed, compared to the previous study [1], the choice of the filtering parameter λ was made prior to GVF-Snake segmentation, thus reducing the number of segmentations to one.

The epicardial segmentation was more difficult to achieve because of the low contrast between myocardium and surrounding structures. The mask was a simple way to prevent the deformable model from any accidental and unnecessary "over-expansion". One simple way to correctly detect the epicardial border was to modify the size of the mask. The main drawback of this constraint was that it required some user intervention. Finally, papillary muscle detection was quite successful using fuzzy k-means clustering and the approach was easy to automate.

Further developments are required to take into account the temporal variations of the myocardial contours during the cardiac cycle. This can be achieved by the adaptation of the 2D+t approach which was recently proposed for aortic segmentation [8]. Moreover, to reduce the manual interactions, the spatial continuity between slices should be better taken into account. These developments should be tested for the “on-line” contest.

One advantage of the proposed approach is that it does not require any specific training. Confirmation was given by the fact that similar results were obtained for both datasets. According to provided results and remarks, difficulty with accurate placement of the contours around the LVOT was shown, but all participants in the challenge suffered from it. The lowest performance was observed for subjects with hypertrophy, whereas results for subjects with ischemic and non-ischemic heart failure and healthy subjects were satisfactory. This challenge provides the opportunity to objectively evaluate several cardiac segmentation algorithms on a single database. Despite some technical difficulties (including the default setting of the GVF-Snake parameters that sometimes needed modification), our segmentation algorithm including myocardial borders and PM detection performed successfully on the provided datasets. Moreover, the usefulness of the segmentation technique presented in this paper on data provided by different centers (different acquisition devices) is currently under investigation [9]. This would potentially allow rendering it robust to image characteristics such as spatial resolution and signal-to-noise ratio.

References

1. El Berbari, R., Kachenoura, N., Redheuil, A., Giron, A., Mousseaux, E., Herment, A., Bloch, I., Frouin, F.: An Automated Estimation of Regional Mean Transition Times and Radial Velocities from Cine Magnetic Resonance Images. Evaluation in Normal Subjects. J Magn Reson Imaging, 30(1): 236-342, (2009), in press
2. MICCAI 2009 Segmentation Challenge, http://smial.sri.utoronto.ca/LV_Challenge/Data.html
3. Radau P., Lu Y., Connelly K., Paul G., Dick A.J., Wright G.A.: Evaluation Framework for Algorithm Segmenting Short Axis Cardiac MRI. The MIDAS Journal-Cardiac MR Left Ventricle Segmentation Challenge, http://hdl.handle.net/10380/3070
4. Constantinides, C., El Berbari, R., De Cesare, A., Chenoune, Y., Roullot, E., Herment, A., Mousseaux, E., Frouin, F., Développement et évaluation d'un algorithme de segmentation automatisée des ventricules gauche et droit sur des images ciné d'IRM . IRBM, (2009), in press
5. Xu, C., Prince, L.J., Snakes, Shapes and Gradient Vector Flow, IEEE Trans. Ima Proc 7:359-69, (1998)
6. Meijster, A., Wilkinson, M., A comparison of algorithms for connected set openings and closings IEEE, Trans Patt Anal Mach Intell, 24, 4:484-94, (2002)
7. Kachenoura N., Redheuil A., Herment A., Mousseaux E., Frouin F.: Robust assessment of the transmural extent of myocardial infarction in late Gadolinium enhanced MRI studies using appropriate angular and circumferential subdivision of the myocardium. Eur Radiol., 18(10): 2140-7, (2008)
8. De Cesare A., Redheuil A., Dogui A., Jolivet O., Lalande A., Frouin F., Mousseaux E., Herment A.: "ART-FUN": an Integrated Software for Functional Analysis of the Aorta. Journal of Cardiovascular Magnetic Resonance, 11(Suppl 1): P182, (2009)
9. Kissi A., Tilmant C., De Cesare A., Comte A., Najman L., Lalande A., Clarysse P., Garreau M., Sarry L., Frouin F.: Initiative Multicentrique pour une Plateforme d’Evaluation en Imagerie Cardiaque. Journées RITS de Recherche en Imagerie et Technologies de la Santé, Lille, (2009)